Quantum interference control of a four-level diamond-configuration quantum system

Han-gyeol Lee, Hyosub Kim, Jongseok Lim, and Jaewook Ahn*
Department of Physics, KAIST, Daejeon 305-701, Korea
(Received 21 June 2013; published 27 November 2013)

We investigate coherent control of the two-photon transition pathways of a four-level atomic system in a diamond configuration. When an ultrashort laser pulse interacts with this system in the ground state $5S_{1/2}$ of rubidium, the two-photon transition probability amplitude of $5D_{3/2}$ is obtained by a summation of all possible resonant and nonresonant two-photon transition probability amplitudes via $5P_{1/2}$ and $5P_{3/2}$. Second-order perturbation theory predicts that the maximal constructive interference of the transition probability amplitudes occurs when the phases of eight different spectrum blocks satisfy four different phase relations. Experiments carried out with spectrally phase-coded laser pulses show good agreement with the theoretical prediction.

DOI: 10.1103/PhysRevA.88.053427 PACS number(s): 32.80.Qk, 32.80.Wr, 42.65.Re

I. INTRODUCTION

Coherent control of light-matter interactions provides a quantum-mechanical means to control the dynamics of a quantum system [1,2]. In particular, coherent control of the broad spectral components of ultrashort laser pulses and their coherent interaction with quantum systems enables the implementation of on-demand quantum interferences among multiple transition passages of the system. Examples of coherent control performed with shaped ultrashort laser pulses are found in experiments [3–10]. Practically important demonstrations of adaptive control, for instance, molecular population transfers and molecular photofragmentations, can be found in [3,4]. The control methods with analytically designed laser pulses have also drawn keen interest among many researchers [7–12].

One of the simplest examples considers a three-level atom in an energy-ladder configuration. When an ultrashort laser pulse interacts with the atom, the second-order time-dependent perturbation theory predicts that the two-photon transition probability amplitude from the ground state $|g\rangle$ to the final state $|f\rangle$ via the intermediate state $|i\rangle$ is given in the perturbative interaction regime by

$$c_{fg}(t) = -\frac{\mu_{fi}\mu_{ig}}{\hbar^2}\int_{-\infty}^{t} dt_1 \int_{-\infty}^{t_1} dt_2 \times E(t_1)E(t_2)e^{i\omega_{fi}t_1+i\omega_{ig}t_2}, \quad (1)$$

where μ_{fi} and μ_{ig} are the dipole moments for the transitions from $|i\rangle$ to $|f\rangle$ and from $|g\rangle$ to $|i\rangle$, respectively, $E(t)$ represents the electric field of the laser pulse, and ω_{ij} is the frequency difference between energy levels i and j. The resulting solution at $t \to \infty$ can be written in the spectral domain as [8]

$$c_{fg} = -\pi\frac{\mu_{fi}\mu_{ig}}{\hbar^2}E(\omega_{ig})E(\omega_{fi}) + i\frac{\mu_{fi}\mu_{ig}}{\hbar^2}\mathrm{P}\int_{-\infty}^{\infty}\frac{E(\omega)E(\omega_{fg}-\omega)}{\omega_{ig}-\omega}d\omega, \quad (2)$$

where $E(\omega)$ is the electric field in the frequency domain, i.e., the Fourier transform of $E(t)$, and P denotes the Cauchy principal value. Using a properly shaped spectral phase function for the laser pulse can enhance the net two-photon transition compared to the result with a transform-limited pulse [8]. The spectral-phase-function solution of a femtosecond pulse, which maximizes the net two-photon transition in the three-level ladder-configuration system, is known as $\phi(\omega) = 0$, $\pi/2$, and 0 for $\omega \in (-\infty,\omega_{ig})$, $(\omega_{ig},\omega_{fi})$, and $(\omega_{fi},+\infty)$, respectively [8]. Likewise, for a three-level V-configuration system, the solution is known as $\phi(\omega) = 0$, $3\pi/2$, and 0 for $\omega \in (-\infty,\omega_{ig})$, $(\omega_{ig},\omega_{fi})$, and $(\omega_{fi},+\infty)$, respectively [13,14].

In this paper, we investigate a four-level diamond-configuration system that comprises a ground state $|g\rangle$, two intermediate states $|a\rangle$ and $|b\rangle$, and a final state $|f\rangle$. In the perturbative interaction regime, the two-photon transition probability amplitude is given by the summation of the two quantum paths via each intermediate state and is written as

$$c_{fg} = -\pi\sum_{i=a,b}\frac{\mu_{fi}\mu_{ig}}{\hbar^2}E(\omega_{ig})E(\omega_{fi}) + i\sum_{i=a,b}\frac{\mu_{fi}\mu_{ig}}{\hbar^2}\mathrm{P}\int_{-\infty}^{\infty}\frac{E(\omega)E(\omega_{fg}-\omega)}{\omega_{ig}-\omega}d\omega. \quad (3)$$

To maximize the given two-photon transition, the two nonresonant transition contributions in the second term in Eq. (3) need to constructively interfere with each other and with the two resonant transitions. In Secs. II and III, we describe a theoretical argument for the spectral-phase-function solution. We provide the experimental demonstration and results in Secs. IV and V and the conclusion in Sec. VI.

II. THEORETICAL CONSIDERATION

The diamond-configuration system comprises the four low-lying energy states, $5S_{1/2}$, $5P_{1/2}$, $5P_{3/2}$, and $5D_{3/2}$, of atomic rubidium [denoted by $|g\rangle$, $|a\rangle$, $|b\rangle$, and $|f\rangle$, respectively; see Fig. 1(a)]. We consider the hyperfine Zeeman sublevels in Sec. III.

To solve the maximal interference problem for the two-photon transition, we decompose the net transition probability amplitude in Eq. (3) into spectral subsets. First, we denote the resonant and nonresonant two-photon contributions as

$$c_{fg} = \sum_{i=a,b} c^{r}_{fg,i} + \sum_{i=a,b} c^{nr}_{fg,i} = c^{r}_{fg} + c^{nr}_{fg}. \quad (4)$$

*jwahn@kaist.ac.kr

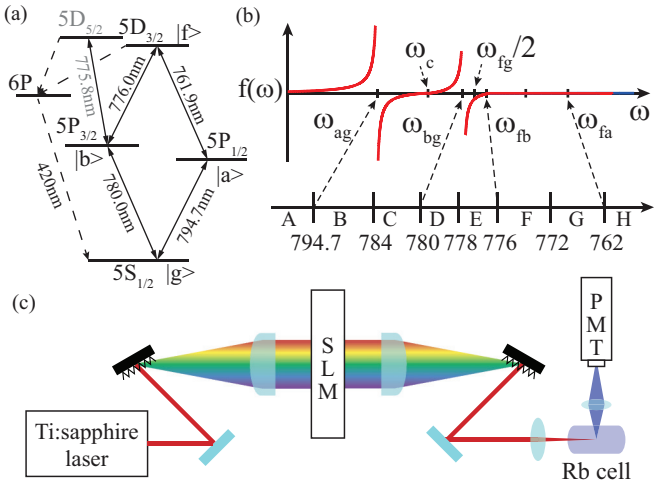

FIG. 1. (Color online) (a) Rubidium energy level configuration [15]. Four states, $5S_{1/2}$, $5P_{1/2}$, $5P_{3/2}$, and $5D_{3/2}$, form a diamond system, while the two-photon transition to $5D_{5/2}$ (gray) via $5P_{3/2}$ forms a ladder system. (b) The spectrum blocks described in Sec. II and the schematic shape of $f(\omega)$, the integrand of c_{fg}^{nr}. (c) Schematic experimental setup.

Each resonant term, $c_{fg,i}^{r}$, is solely contributed by the two-photon resonant spectral components of the laser pulse, so the amplitude of $c_{fg,i}^{r}$ is not affected by the spectral phase function. However, the nonresonant terms, $c_{fg,i}^{nr}$, are integrated over the whole spectral range, and therefore, they sensitively respond to the spectral phase function.

Let us assume that the spectral phase of the laser pulse is constant over the whole spectrum. For convenience, we define $f(\omega)$, the integrand of the total nonresonant part c_{fg}^{nr}, as

$$f(\omega) = \sum_{i=a,b} \frac{\mu_{fi}\mu_{ig}}{\hbar^2} \frac{E(\omega)E(\omega_{fg}-\omega)}{\omega_{ig}-\omega}, \tag{5}$$

where the imaginary unit i is omitted from $f(\omega)$ because the relative phase between the resonant and nonresonant parts is not important here. Then, $f(\omega)$ changes its phase at resonant frequency ω_{ig} due to the change in the sign of the denominator $\omega_{ig}-\omega$ across the resonance for each pathway, $|g\rangle \to |a\rangle \to |f\rangle$ and $|g\rangle \to |b\rangle \to |f\rangle$. The interference between the two pathways introduces another critical frequency, ω_c, where $f(\omega)$ changes its sign [see Fig. 1(b)]. ω_c is located between ω_{ag} and ω_{bg} and is defined as

$$\omega_c = \frac{k\omega_{ag}+\omega_{bg}}{k+1}, \qquad k = \frac{\mu_{fb}\mu_{bg}}{\mu_{fa}\mu_{ag}}. \tag{6}$$

Finally, a photon pair that makes up a two-photon transition satisfies the frequency-sum relation, $\omega_{fg} = \omega_1 + \omega_2$, which appears in the numerator of $f(\omega)$, $E(\omega)E(\omega_{fg}-\omega)$. Because the spectral components are symmetrically added around $\omega_{fg}/2$, the spectral boundaries are also symmetric around $\omega_{fg}/2$. Hence, there are seven spectral boundaries, ω_{ag}, ω_c, ω_{bg}, $\omega_{fg}/2$, ω_{fb}, $\omega_{fg}-\omega_c$, and ω_{fa}, making eight spectrum blocks divided by the boundaries. Within each block, the phase of $f(\omega)$ is the same if the given spectral block has a constant phase.

To be more specific, we denote the eight spectrum blocks as $A = (-\infty,\omega_{ag})$, $B = (\omega_{ag},\omega_c)$, $C = (\omega_c,\omega_{bg})$, $D = (\omega_{bg},\omega_{fg}/2)$, $E = (\omega_{fg}/2,\omega_{fb})$, $F = (\omega_{fb},\omega_{fg}-\omega_c)$, $G = (\omega_{fg}-\omega_c,\omega_{fa})$, and $H = (\omega_{fa},\infty)$ and also define the positive-definite functions $\alpha(\omega)$ and $\beta(\omega)$ as

$$\alpha(\omega) = \frac{\mu_{fa}\mu_{ag}}{\hbar^2}\frac{|E(\omega)E(\omega_{fg}-\omega)|}{|\omega_{ag}-\omega|}, \quad \beta(\omega) = \frac{\mu_{fb}\mu_{bg}}{\hbar^2}\frac{|E(\omega)E(\omega_{fg}-\omega)|}{|\omega_{bg}-\omega|}. \tag{7}$$

Then, the nonresonant part c_{fg}^{nr} in Eq. (4) is given as

$$\begin{aligned} -ic_{fg}^{nr} = &\left[\int_A \alpha(\omega)d\omega + \int_A \beta(\omega)d\omega - \int_H \alpha(\omega)d\omega - \int_H \beta(\omega)d\omega\right] e^{i\phi_A} e^{i\phi_H} \\ &- \left[\int_B \alpha(\omega)d\omega - \int_B \beta(\omega)d\omega + \int_G \alpha(\omega)d\omega + \int_G \beta(\omega)d\omega\right] e^{i\phi_B} e^{i\phi_G} \\ &+ \left[\int_C \beta(\omega)d\omega - \int_C \alpha(\omega)d\omega - \int_F \alpha(\omega)d\omega - \int_F \beta(\omega)d\omega\right] e^{i\phi_C} e^{i\phi_F} \\ &- \left[\int_D \beta(\omega)d\omega + \int_D \alpha(\omega)d\omega + \int_E \alpha(\omega)d\omega + \int_E \beta(\omega)d\omega\right] e^{i\phi_D} e^{i\phi_E}, \end{aligned} \tag{8}$$

where ϕ_i denotes the phase of spectrum block i. Note that the first term in each square bracket in Eq. (8) indicates the dominant term in each spectrum block, as the function $\alpha(\omega)$ or $\beta(\omega)$ in Eq. (7) shows singular behavior as ω approaches ω_{ag} or ω_{bg}, respectively.

As found in Eq. (8), not all of the phases $\{\phi_A,\phi_B,\ldots,\phi_H\}$ are independently controlled. Therefore, we use the first four phases, A to D, and leave the other four phases, E to H, as zero. By substituting the spectrum of the laser pulse, Eq. (8) becomes

$$c_{fg}^{nr} = i\,[c_A e^{i\phi_A} - c_B e^{i\phi_B} + c_C e^{i\phi_C} - c_D e^{i\phi_D}], \tag{9}$$

where c_j for $j \in \{A,B,C,D\}$ is the sum of the integrals in each square bracket of Eq. (8), labeled with its dominant spectrum block j. As all the c_j's are positive, the maximal c_{fg}^{nr} is obtained when the following relations are satisfied:

$$\phi_A = \phi_C = \phi_B + \pi = \phi_D + \pi. \tag{10}$$

III. HYPERFINE TRANSITIONS

The four energy levels of atomic rubidium have a total of 12 hyperfine levels, $F = 2,3$ for $5S_{1/2}$, $F' = 2,3$ for $5P_{1/2}$, $F' = 1,2,3,4$ for $5P_{3/2}$, and $F'' = 1,2,3,4$ for $5D_{3/2}$. To calculate the transition probability amplitude in Eq. (3), we need to consider all of the individual hyperfine transitions. The hyperfine transition dipole moments are calculated using the reduction formulas [16–18], $\langle F,m_F|er_q|F',m_{F'}\rangle = \langle F||er||F'\rangle\langle F,m_F|F',1,m_{F'},q\rangle$ and

$$\begin{aligned}\langle F||er||F'\rangle &= \langle JIF||er||J'I'F'\rangle \\ &= \langle J||er||J'\rangle(-1)^{F'+J+1+I}\begin{Bmatrix} J & J' & 1 \\ F' & F & I \end{Bmatrix}, \end{aligned} \tag{11}$$

where the nuclear spin $I = 5/2$ for ^{85}Rb. We limit our calculation to $\Delta m_F = 0$ as our experiment uses linearly polarized light. We also assume that there is no external magnetic field, i.e., all Zeeman sublevels are degenerate. Taking into account the hyperfine splitting, the transition probability amplitude from a ground sublevel $(F,\, m_F)$ to a final sublevel $(F'',\, m_F)$ is described by

$$\begin{aligned} c_{F''F,m_F} &= -\pi\sqrt{P_{F,m_F}}\sum_{J',F'_{J'}}\frac{\mu_{F''F'_{J'},m_F}\mu_{F'_{J'}F,m_F}}{\hbar^2} \\ &\quad\times E(\omega_{F''F'_{J'}})E(\omega_{F'_{J'}F}) \\ &\quad + i\sqrt{P_{F,m_F}}\sum_{J',F'_{J'}}\frac{\mu_{F''F'_{J'},m_F}\mu_{F'_{J'}F,m_F}}{\hbar^2} \\ &\quad\times \mathrm{P}\int_{-\infty}^{\infty}\frac{E(\omega)E(\omega_{F''F}-\omega)}{\omega_{F'_{J'}F}-\omega}d\omega, \end{aligned} \tag{12}$$

where P_{F,m_F} is the statistical probability of the ground sublevels (F,m_F) and $\mu_{F'_{J'}F,m_F}$ is the transition dipole moment for $(F,m_F) \to (F'_{J'},m_F)$. $F'_{J'}$ indicates the hyperfine state F' of J', and the J' summation denotes the sum of all possible two-photon transitions via $5P_{1/2}$ and $5P_{3/2}$. Then, the resulting transition probability from $5S_{1/2}$ to $5D_{3/2}$ is given by

$$P_{5S_{1/2}\to 5D_{3/2}} = \sum_{F'',F,m_F}|c_{F''F,m_F}|^2. \tag{13}$$

However, as $E(\omega)$ is slowly varying and the hyperfine sublevels are nearly energy degenerate for far-off resonant components, Eq. (12) can be simplified as

$$\begin{aligned} c_{F''F,m_F} &\approx -\pi\sqrt{P_{F,m_F}}\sum_{i=a,b}\frac{\mu^{(2)}_{F''F,m_F,J'(i)}}{\hbar^2}E(\omega_{fi})E(\omega_{ig}) \\ &\quad + i\sqrt{P_{F,m_F}}\sum_{i=a,b}\frac{\mu^{(2)}_{F''F,m_F,J'(i)}}{\hbar^2}\int_{|\omega-\omega_{ig}|\gg 0} \\ &\quad\times\frac{E(\omega)E(\omega_{fg}-\omega)}{\omega_{ig}-\omega}d\omega + S, \end{aligned} \tag{14}$$

where $\mu^{(2)}_{F''F,m_F,J'(i)} = \sum_{F'_{J'(i)}}\mu_{F''F'_{J'(i)},m_F}\mu_{F'_{J'(i)}F,m_F}$ for $i = a,b$ is the sum of two-photon transition dipole moments via all possible $J'(i)$ states. Here, S is the spectral integral near the hyperfine resonance region, which remains constant in our experiments because of the limited spectral resolution. Strikingly, the numerical calculation finds the fixed ratio between $\mu^{(2)}_{F''F,m_F,J'(a)}$ and $\mu^{(2)}_{F''F,m_F,J'(b)}$, or

$$\frac{\mu^{(2)}_{F''F,m_F,J'=3/2}}{\mu^{(2)}_{F''F,m_F,J'=1/2}} = \frac{\sqrt{3}}{5}, \tag{15}$$

the result of which is also independent of m_F. Therefore, Eq. (14) is simply reduced to Eq. (3), and even if hyperfine transitions are considered, ω_c in Eq. (6) is a constant for all possible F and F'' pairs.

IV. EXPERIMENTAL DESCRIPTION

For the experiment, broadband laser pulses were produced by a Ti:sapphire mode-locked laser oscillator operating at a repetition rate of 80 MHz and were then spectrally programmed by a spatial light modulator (SLM) [see Fig. 1(c)] [19]. The laser spectrum was centered at 782 nm, close to the two-photon resonant wavelength of 778 nm. The SLM with 128 liquid-crystal pixels was located in the Fourier plane of the $4f$ geometry zero-dispersion Martinez stretcher [20] with a pair of cylindrical lenses ($f = 100$ mm) and a pair of gratings (1200/mm). The spectral resolution per pixel for a liquid crystal cell unit 97 μm wide with 3-μm spacing was 0.5 nm, so the spectral region of each rubidium resonant level was excluded from the phase shaping. The shaped laser pulses, with energy up to 0.5 nJ, were focused by a lens with a focal length of 75 mm inside the rubidium vapor cell, and the fluorescence signal at 420 nm via $6P$ was collected by a photomultiplier tube. The collected signal did not exclude the two-photon transition to $5D_{5/2}$ due to the small splitting between the two 5D states. However, the ladder transition to $5D_{5/2}$, which is only sensitive to the spectral blocks C and D, did not interfere with the diamond transitions to $5D_{3/2}$ in the perturbative interaction regime. A brief estimation of the pulse area $\int_{-\infty}^{\infty}\mu A(t)/\hbar dt \sim 0.1$, where $A(t)$ is the electric field envelope, calculated with an estimated peak electric field of 5 MV/m and pulse duration of 100 fs, confirms that the interaction is in the perturbative regime [21]. To observe the quantum interference between the two excitation passages, $|g\rangle \to |a\rangle \to |f\rangle$ and $|g\rangle \to |b\rangle \to |f\rangle$, laser pulses with a wide spectral width, about 45 nm FWHM, were required due to the energy difference (15 nm) between $|a\rangle$ and $|b\rangle$.

Phase-step scanning. Before proceeding to the quantum interference experiment, we performed a phase-step scanning experiment. The laser pulse was spectrally shaped with a phase function $\phi(\lambda) = \pi\Theta(\lambda - \lambda_s)$, where $\Theta(\lambda)$ is the Heaviside step function and λ_s changes through the laser spectrum. As shown in Fig. 2(a), the π-phase step was swept to calibrate the spectral position of the SLM pixels. When the π-phase step was located at a resonant frequency, it inverted the base sign of the nonresonant transition probability amplitude in Eq. (3), and part of the destructive interference was removed. As a result, at each resonant frequency position, the two-photon transition probability increased, and a sharp peak occurred. Figure 2(b) shows the experimental results of the phase-step sweeping and identifies the rubidium resonant-level locations in the SLM.

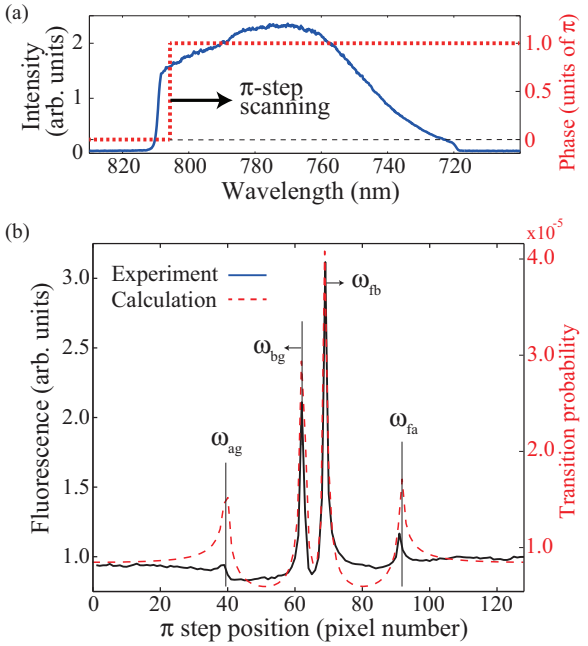

FIG. 2. (Color online) Phase-step scanning experiment: (a) Laser spectrum after the SLM (solid line) and phase-step function (dashed line), where the spectral tails were cut for better spectral resolution. (b) The fluorescence signal (solid line) obtained by sweeping the spectral π-phase step, overlaid with the numerical calculation (dashed line). Each peak is labeled with the corresponding resonant frequency.

V. RESULTS

The phase programming of spectrum blocks aims to control the interference between the two passages of rubidium two-photon transition from $|g\rangle$ to $|f\rangle$. Assume that the laser pulse has a constant phase over the spectrum. Then, as described in Eq. (9), destructive interference occurs due to the base phase differences in the transition probability amplitude components. We can represent this behavior in a vector diagram, as in Fig. 3(a). The phases of the resonant and nonresonant transition probability amplitude components are shown as vectors, with the proper labeling introduced in Eq. (9). For convenience, we define

$$c_+^{nr} = c_A e^{i\phi_A} + c_C e^{i\phi_C}, \qquad c_-^{nr} = c_B e^{i\phi_C} + c_D e^{i\phi_D}. \quad (16)$$

$A + C$ phase rotation. The first experiment considered the interference control of A and C with respect to $B + D$ and the resonant components. The vector diagram in Fig. 3(b) shows the schematics of this experiment, where we applied a $-\pi/2$ to 2π phase to A and C independently with $\pi/10$ steps. As the phase increased, the nonresonant components corresponding to A and C rotated counterclockwise, and the initial destructive interference was gradually removed. Figure 3(d) shows the result. As the phases of A and C respectively reached $\pi/2$, the two-photon transition probability increased and a maximum occurred. Note that the maximum point shifted toward π in both the ϕ_A and ϕ_C directions because of the other nonresonant components B and D, in which the phase differences with respect to A and C are inherently π.

$B + C$ phase rotation. The second experiment used the phases of B and C to control the interference with respect to

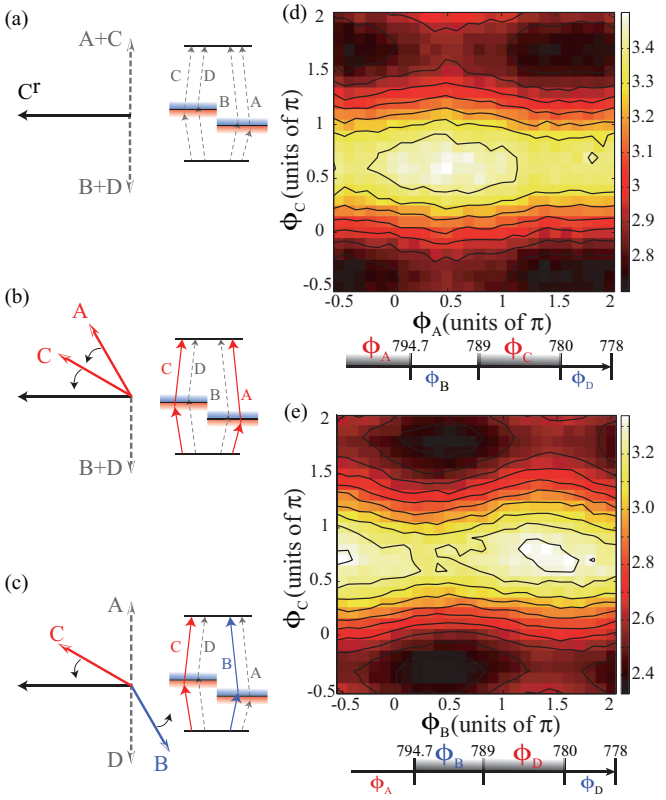

FIG. 3. (Color online) (a) Vector diagram for the resonant (C^r) and nonresonant ($A + C$, $B + D$) transitions. (b) $A + C$ phase rotation. (c) $B + C$ phase rotation. (d) Experimental result for (b), where the phases ϕ_A and ϕ_C are independently varied from $-\pi/2$ to 2π. (e) Experimental result for (c), where ϕ_B and ϕ_C are independently varied from $-\pi/2$ to 2π.

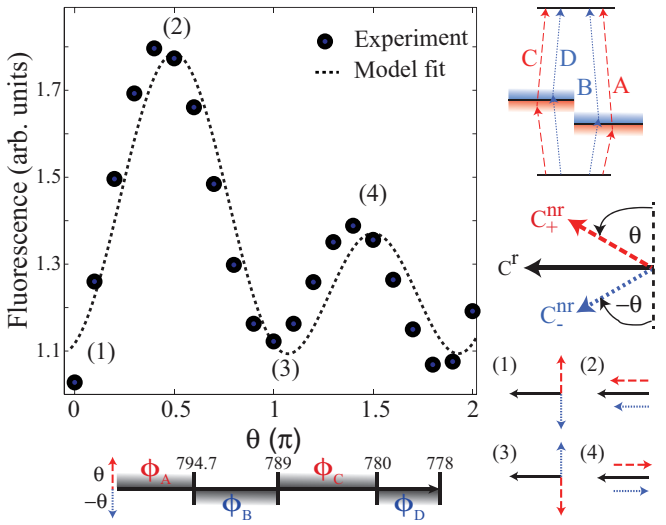

FIG. 4. (Color online) Interference control of all nonresonant components with respect to the resonant component. The phases of A and C vary from 0 to 2π, while the phases of B and D vary simultaneously from 0 to -2π. The vector diagrams in the bottom right corner show the orientation of each transition probability amplitude component corresponding to the numbered points in the main plot.

TABLE I. Phase function solution of the four-level diamond-configuration system.

	Block							
	A	*B*	*C*	*D*	*E*	*F*	*G*	*H*
ω	$(-\infty,\omega_{ag})$	(ω_{ag},ω_c)	(ω_c,ω_{bg})	$(\omega_{bg},\frac{\omega_{fg}}{2})$	$(\frac{\omega_{fg}}{2},\omega_{fb})$	$(\omega_{fb},\omega_{fg}-\omega_c)$	$(\omega_{fg}-\omega_c,\omega_{fa})$	(ω_{fa},∞)
$\phi(\omega)$	$\frac{\pi}{2}-\phi_H$	$-\frac{\pi}{2}-\phi_G$	$\frac{\pi}{2}-\phi_F$	$-\frac{\pi}{2}-\phi_E$	ϕ_E	ϕ_F	ϕ_G	ϕ_H

$A+D$ and the resonant component. The vector diagram in Fig. 3(c) describes the concept of this experiment. For this, we applied a $-\pi/2$ to 2π phase to B and C independently with $\pi/10$ steps. Unlike in the previous case of A and C control, B and C were initially in opposite directions from each other, or with the phase difference of π. Hence, the maximal occurred near $\phi_B=\pi/2$ and $\phi_C=3\pi/2$, as shown in Fig. 3(e).

$AC+BD$ phase rotation. Finally, we applied interference control to all nonresonant components with respect to the resonant component. Direct phase shaping of a resonant frequency component was not available via our SLM due to the limit of the frequency resolution. Therefore, we controlled the nonresonant components to align them with the resonant one. In this experiment, θ, the phase of A and C, which has an inherent phase of $\pi/2$, was simultaneously varied from 0 to 2π, while the phase of B and D, which has an inherent phase of $3\pi/2$, was varied from 0 to -2π, i.e., $-\theta$. Then, as described in Fig. 4, the nonresonant component c_+^{nr} rotated counterclockwise, and c_-^{nr} rotated clockwise. After $\theta=\pi/2$ rotation, the two nonresonant components and the resonant component were all aligned, and the maximal transition probability was achieved. Another local maximum occurred at $\theta=3\pi/2$ as a consequence of the antiparallel resonant and nonresonant components. Figure 4 shows the experimental results of the interference control. The data were fitted with the empirical formula

$$c_{fg}=-r+xe^{i(\theta+\pi/2)}+ye^{i(-\theta-\pi/2)}, \tag{17}$$

where r is $|c_{fg}^r|$, x is $|c_+^{nr}|$, y is $|c_-^{nr}|$, and θ is the phase applied to the spectrum blocks. The result confirms the phase function solution summarized in Table I, that A and C should be $\pi/2$ phase shifted from resonant transitions and π phase shifted from B and D.

VI. CONCLUSION

In summary, we considered the coherent control of the four-level ($5S_{1/2}$, $5P_{1/2}$, $5P_{3/2}$, and $5D_{3/2}$) diamond-configuration system of atomic rubidium. The second-order perturbation theory predicts that the phase function solution satisfying the maximal constructive interference of the two two-photon transition pathways from $5S_{1/2}$ to $5D_{3/2}$ is obtained as four relations of $\phi_A+\phi_H=\pi/2$, $\phi_B+\phi_G=-\pi/2$, $\phi_C+\phi_F=\pi/2$, and $\phi_D+\phi_E=-\pi/2$, where ϕ_A, ϕ_B, . . . , and ϕ_H are the uniform phases of the eight spectrum blocks given in Sec. II. Experiments performed with spectrally phase-shaped femtosecond laser pulses confirmed the obtained phase function solution.

ACKNOWLEDGMENTS

This research was supported in part by Basic Science Research Programs (Grants No. 2013R1A2A2A05005187 and No. 2009-0093428) and in part by the WCI Program (Grant No. WCI 2011-001) through the National Research Foundation of Korea. The authors thank Heung-Sun Sim and Gi-hyun Go for fruitful discussion.

[1] B. W. Shore, *Manipulating Quantum Structures Using Laser Pulses* (Cambridge University Press, New York, 2011).
[2] M. Shapiro and P. Brumer, *Principles of the Quantum Control of Molecular Processes* (Wiley, New York, 2003).
[3] C. J. Bardeen, J. Che, K. R. Wilson, V. V. Yakovlev, P. Cong, B. Kohler, J. L. Krause, and M. Messina, J. Phys. Chem. A **101**, 3815 (1997).
[4] A. Assion, T. Baumert, M. Bergt, T. Brixner, B. Kiefer, V. Seyfried, M. Strehle, and G. Gerber, Science **282**, 919 (1998).
[5] S. Cialdi, M. Petrarca, and C. Vicario, Opt. Lett. **31**, 2885 (2006).
[6] M. C. Stowe, A. Pe'er, and J. Ye, Phys. Rev. Lett. **100**, 203001 (2008).
[7] D. Meshulach and Y. Silberberg, Phys. Rev. A **60**, 1287 (1999).
[8] N. Dudovich, B. Dayan, S. M. Gallagher Faeder, and Y. Silberberg, Phys. Rev. Lett. **86**, 47 (2001).
[9] S. D. Clow, C. Trallero-Herrero, T. Bergeman, and T. Weinacht, Phys. Rev. Lett. **100**, 233603 (2008).
[10] M. Viteau, A. Chotia, M. Allegrini, N. Bouloufa, O. Dulieu, D. Comparat, and P. Pillet, Science **321**, 232 (2008).
[11] S. Lee, J. Lim, J. Ahn, V. Hakobyan, and S. Guerin, Phys. Rev A **82**, 023408 (2010).
[12] S. Lee, J. Lim, C. Y. Park, and J. Ahn, Opt. Express **19**, 2266 (2011).
[13] J. Lim, H. G. Lee, J. U. Kim, S. Lee, and J. Ahn, Phys. Rev. A **83**, 053429 (2011).
[14] J. Lim, H. G. Lee, S. Lee, and J. Ahn, Phys. Rev. A **84**, 013425 (2011).
[15] J. E. Sansonetti, J. Phys. Chem. Ref. Data **35**, 301 (2006).
[16] D. M. Brink and G. R. Satchler, *Angular Momentum* (Oxford University Press, London, 1968).
[17] D. A. Steck, Rubidium 85 D line data, http://steck.us/alkalidata, rev. 2.1.5, 19 September 2012.
[18] F. Nez, F. Biraben, R. Felder, and Y. Millerioux, Opt. Commun. **102**, 432 (1993).
[19] A. M. Weiner, Rev. Sci. Instrum. **71**, 1929 (2000).
[20] R. L. Fork, O. E. Martinez, and J. P. Gordon, Opt. Lett. **9**, 150 (1984).
[21] J. Lim, K. Lee, and J. Ahn, Opt. Lett. **37**, 3378 (2012).